Global Energy Interconnection 8 (2025) 460–473

KeAi
CHINESE ROOTS
GLOBAL IMPACT

Global Energy Interconnection
Development and Cooperation Organization

Global Energy Interconnection

Contents lists available at ScienceDirect
journal homepage: www.elsevier.com/locate/gloei

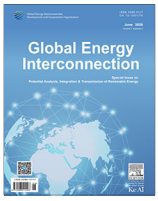

Assessing the capacity value of demand flexibility from aggregated small Internet data centers in power distribution systems

Bo Zeng, Xinzhu Xu *, Fulin Yang

State Key Laboratory of Alternate Electrical Power System with Renewable Energy Sources, North China Electric Power University, Beijing 102206, China

Received 26 June 2024; revised 29 July 2024; accepted 18 August 2024

Abstract

With the advent of the digital economy, there has been a rapid proliferation of small-scale Internet data centers (SIDCs). By leveraging their spatiotemporal load regulation potential through data workload balancing, aggregated SIDCs have emerged as promising demand response (DR) resources for future power distribution systems. This paper presents an innovative framework for assessing capacity value (CV) by aggregating SIDCs participating in DR programs (SIDC-DR). Initially, we delineate the concept of CV tailored for aggregated SIDC scenarios and establish a metric for the assessment. Considering the effects of the data load dynamics, equipment constraints, and user behavior, we developed a sophisticated DR model for aggregated SIDCs using a data network aggregation method. Unlike existing studies, the proposed model captures the uncertainties associated with end tenant decisions to opt into an SIDC-DR program by utilizing a novel uncertainty modeling approach called Z-number formulation. This approach accounts for both the uncertainty in user participation intentions and the reliability of basic information during the DR process, enabling high-resolution profiling of the SIDC-DR potential in the CV evaluation. Simulation results from numerical studies conducted on a modified IEEE-33 node distribution system confirmed the effectiveness of the proposed approach and highlighted the potential benefits of SIDC-DR utilization in the efficient operation of future power systems.

Keywords: Aggregated Small internet data center; Demand response; Capacity value; Z-number

0 Introduction

In recent years, the Internet data center (IDC) market has experienced robust expansion, with its value surpassing 220 billion yuan in China, signaling a shift toward a computing-power-centric development phase. Future projections show a stabilization in the growth of major Internet clientele, with rising demand from mid-tier sectors such as finance, government, and manufacturing. This shift has increased the prevalence of small-scale data centers. Meanwhile, because computing resources are strategically reallocated from eastern to western China, Internet service companies can establish multiple IDCs to provide large-scale services. Leveraging the flexibility of data centers in this evolving context enhances efficiency and reduces energy consumption, helping to mitigate significant grid connection challenges [1].

From the perspective of the demand-side potential, scholars have conducted extensive research on the characteristics of the spatiotemporal load of IDCs. Reference. [2] defines the demand response (DR) potential of a data center as the power transfer in time and space caused by a delay-tolerant central processing unit when processing a large volume of data. Ref. [3] proposed a new method of spatial and temporal redistribution for the energy management of edge IDC clusters based on IDCs participating in DR (IDC-DR). Refs. [26] and [27] made use of various load characteristics within the IDC and the potential of

* Corresponding author.
E-mail addresses: alosecity@126.com (B. Zeng), 18686228775@163.com (X. Xu), notyour@126.com (F. Yang).

https://doi.org/10.1016/j.gloei.2024.08.013

IDC-DR to improve the economy of IDC operation. Because the data load flow between IDCs is the power demand flow of the node where the IDCs are located [5], each data network can be represented as a virtual power grid (VPG). Several studies have been conducted for a virtual power grid that participates in DR projects (VPG-DR). A model that can accurately calculate a VPG-DR and the simulation results prove that a VPG-DR can help lower the power system operation costs and increase social welfare [6]. However, most existing research focuses on large IDC-DRs; small IDCs cannot directly participate in DR because of their size limitations. To address this problem, a method of aggregating small VPGs was proposed to extend IDC-DR to more IDCs, which aligns with the future development trend of IDCs [6].

The capacity value (CV) of IDC-DR has not been accurately described as a unique flexible resource on the demand side. Therefore, in this study, we introduce the CV concept into a small-scale IDC (SIDC). CV was first introduced to measure the capability of renewable energy sources to contribute to the overall capacity of power systems [7]. Owing to the uncertainty of renewable energy, it is of great significance to evaluate the CV of renewable energy before it is connected to the grid for the safe and reliable operation of the power system. Some studies have already calculated the CV of common renewable energy sources, such as wind turbines and solar energy [9], and this concept has also been extended to more application scenarios, such as the calculated CV of energy storage [8]. With the gradual promotion of new power systems, scholars have extended the CV concept and applied it to the demand side. For example, a comprehensive multistage programming model was proposed to investigate the potential capability of DR for the reliable operation of a distribution grid [11]. Ref. [12] puts forward a method for evaluating the CV of large IDCs.

The participation of SIDCs in DR is often overlooked because of their limited individual impact and cost-effectiveness concerns regarding the IDC and power grid [13]. This oversight has resulted in a scarcity of research assessing their capacity to contribute to DR. Despite this, the burgeoning number of SIDCs, fueled by their growth, presents an opportunity. The concept of aggregated SIDCs (ASIDCs) has emerged as a viable solution, enabling these smaller entities to collectively participate in DR. However, current studies neglect the uncertainties in user participation and the inherent variability of data within IDCs, thus not fully capturing their potential in this domain. This gap highlights the need for a specialized CV assessment method for smaller centers. By functioning as virtual energy storage resources within an aggregated framework, SIDC clusters can significantly enhance the reliability and stability of power supply systems. In this context, accurately evaluating the DR capacity of SIDCs is pivotal, and offers crucial insights for grid operators to develop effective incentive policies and steer the energy use patterns of SIDCs.

The major contributions of this paper are as follows:

(1) To characterize the demand flexibility of SIDCs, an aggregate model was used to represent their participation in DR programs and their impact on the power grid.
(2) This study defines CV within the context of SIDCs participating in DR programs (SIDC-DR), providing a fair and visual framework for comparing the reliability of generation- and demand-side resources. This framework enables utility operators to estimate the potential reliability benefits of SIDC-DR programs under various scenarios without excessive computational complexity.
(3) Considering the demand responsivity is influenced by the data load characteristics and user willingness to participate in SIDC-DR programs, a novel SIDC-DR model based on a Z-number representation is proposed. This model explicitly addresses the information credibility issue, enabling a more accurate and comprehensive characterization of the stochastic nature of SIDC demand flexibility.

The remainder of this paper is organized as follows. Section "Definition of CV in SIDC-DR" provides an overview of the system and its key definitions. Section "IDC-DR modeling" outlines the model formulation and Section "IDC-DR capacity value assessment" details the methodology. Numerical studies are discussed in Section "Case analysis", and the conclusions are presented in Section "Conclusion".

1 Definition of CV in SIDC-DR

1.1 System overview

This study investigates an electrical framework comprising generator units, transmission lines, consumer demand, and SIDCs. The primary energy source for this system is the generator unit, with external grid power via transformers acting as a backup for critical situations. Fig. 1 presents a typical basic architecture diagram of a power grid that includes SIDCs, illustrating the coupling relationship between the power grid and computing network, as well as the ASIDC model. The right side of Fig. 1 displays the SIDC physical composition and load types, revealing that the SIDCs consist of IT servers, air conditioning equipment, and auxiliary equipment. The bottom right figure shows how SIDCs leverage the spatiotemporal flexibility of certain loads to participate in DR. Energy is distributed to consumers, and data from consumers are processed by the SIDC. SIDC management adjusts the computational controls based on data

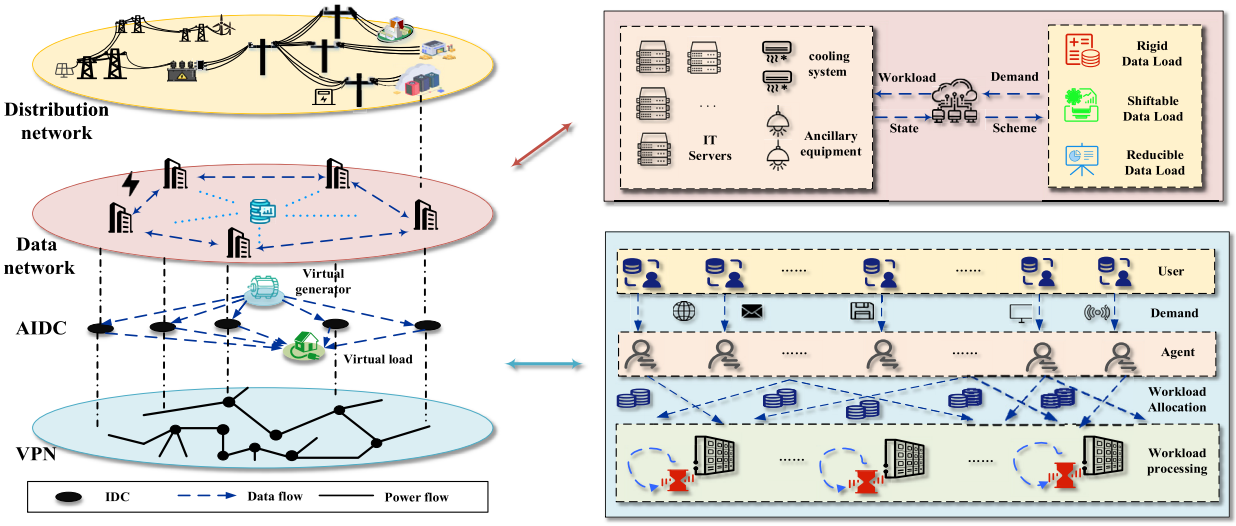

Fig. 1. Electrical system architecture with SIDC.

attributes and grid requirements to ensure efficient load management. During power shortages, the SIDC can lower consumption by prioritizing information processing. This study assumes 100 % reliability for transmission lines, excluding malfunction scenarios [15], simplifying the modeling process and ensuring the accuracy of capacity benefit assessments without adding complexity.

1.2 CV indicator definition

In a power system, CV refers to the effective installed capacity contributed by the power generation equipment to satisfy the reliability requirements of the system [10]. Similar to the traditional capacity assessment of power generation sources, the CV of an IDC equipped with DR capabilities, functioning as a virtual power generation resource, can also be conceptualized through the introduction of the term CV.

In this study, we adopt equivalent conventional capacity (ECC) as a measure for evaluating the DR capacity of SIDCs. ECC is defined as the capacity of conventional generator sets, which an IDC-DR can replace within a certain period, while simultaneously preserving consistent reliability levels within the power system. The mathematical expression for the ECC is as follows:

$$\mathbb{R}_{\text{system}}[(C^{\text{g}}+C_{\text{IDC}});D]=\mathbb{R}_{\text{target}}[(C^{\text{g}}+E_{\text{CC}});D] \tag{1}$$

where D is the demand value of electrical loads, $\mathbb{R}$ is the reliability index of the distribution system, denoted as the expected energy not supplied (EENS), and is selected as the reliability indicator for the power supply in this study. $\mathbb{R}_{\text{system}}$ is the reliability index of a power system and is often represented as the power supply reliability. $\mathbb{R}_{\text{target}}$ is the target reliability level, which is the desired reliability standard for a system. C^{g} denotes the total power generated by the system. C_{IDC} is the installed capacity of the IDCs. Eq. (1) indicates that when the existing generation capacity that provides C^{g} in the system is combined with the E_{CC} to satisfy the power demand D, the system reliability will achieve the target reliability level R_{target}.

The EENS refers to the anticipated energy that remains unfulfilled owing to insufficient electrical supply in the power system caused by various factors, leading to unmet user demand [14]. The formula for EENS is as follows:

$$E_{\text{ENS}}=1/N\sum_{t=1}^{8760\times N}E_{\text{NS}t} \tag{2}$$

$$E_{\text{NS}t}=\begin{cases}0, b_t^{\text{usd}}=0\\ P_t^{\text{usd}}, b_t^{\text{usd}}=1\end{cases}\forall t\in T \tag{3}$$

where N is the number of simulation years, $E_{\text{NS}t}$ signifies the deficit in electricity consumption compared with the expected value during time period t, and b_t^{usd} is a binary state variable that takes values of 0 or 1. During instances of load shedding within the system in that timeframe ($b_t^{\text{usd}}=1$), P_t^{usd} represents the corresponding power loss due to load shedding; otherwise, it is equal to zero.

2 IDC-DR modeling

2.1 IDC energy consumption characteristics

As delineated in the preceding sections, the energy consumption of the SIDC is predominantly attributed to three components: servers, air conditioning apparatus, and other ancillary equipment [4]. Consequently, the overall power consumption of an operational SIDC can be expressed as

$$P_{c,n,t}^{\text{SIDC}}=P_{c,n,t}^{\text{SIDC - Ser}}+P_{c,n,t}^{\text{SIDC - ACS}}+P_{c,n,t}^{\text{o-e}} \tag{4}$$

where $P_{c,n,t}^{\mathrm{SIDC-Ser}}$, $\mathrm{P}_{\mathrm{c,n,t}}^{\mathrm{SIDC\text{-}ACS}}$, and $\mathrm{P}_{\mathrm{c,n,t}}^{\mathrm{o\text{-}e}}$ represents the active power consumption of the servers, air conditioning equipment, and other equipment within the SIDC, respectively.

In the data center (DC) framework, the energy consumption of the servers is principally determined by the number of active servers during the current time interval and the volume of information task loads. This study operates under the assumption that all servers housed within the DC have a uniform model and that any informational load during a given interval is evenly distributed among all the powered-on servers. Given that the quiescent power consumption of a singular server when not processing tasks is denoted as $\mathrm{P_{idle}}$ and its peak power is denoted as $\mathrm{P_{peak}}$, the power consumption characteristics under various operational conditions are elucidated as follows, according to reference [18]:

$$P_{c,n,t}^{\mathrm{SIDC\text{-}Ser}} = N_{\mathrm{umc},n,t}^{\mathrm{Ser\text{-}on}} P_{c,n,t}^{\mathrm{Ser\text{-}min}} + \left(P_{c,n,t}^{\mathrm{Ser\text{-}max}} - P_{c,n,t}^{\mathrm{Ser\text{-}min}}\right)\varphi_d N_{\mathrm{um}\ c,n,t}^{\mathrm{Ser\text{-}on}} \tag{5}$$

$$\varphi_d = W_{\mathrm{Lc},n,t}/N_{\mathrm{umc},n,t}^{\mathrm{Ser\text{-}on}}\mu_d \tag{6}$$

$$0 \leqslant N_{\mathrm{umc},n,t}^{\mathrm{Ser\text{-}on}} \leqslant (1-\phi)N_{\mathrm{umc},n}^{\mathrm{Ser}} \tag{7}$$

$$0 \leqslant \varphi_d \leqslant U_{\max} \tag{8}$$

Eqs. (5)–(8) depict the power consumption computation for an individual server, constraints on the number of powered-on servers in the DC, and constraints pertaining to the server CPU utilization rate. In this context, μ_{d} denotes the average utilization rate of the server. $N_{\mathrm{umc},n,t}^{\mathrm{Ser\text{-}on}}$ represents the number of servers in an active state during time interval t. $W_{\mathrm{Lc},n,t}$ stands for the data task volume within the DC. φ_{d} symbolizes the processing rate of the server.$\mathrm{n_d^{Ser}}$ indicates the configured number of servers. ϕ corresponds to the server redundancy factor. $U_{\max}$ elucidates the upper limit of the CPU utilization rate for an individual server.

The operational characteristics of the air conditioning system can be expressed as follows:

$$P_{c,n,t}^{\mathrm{IDC\text{-}ACS}} = H_{c,n,t}^{\mathrm{IDC\text{-}ACS}}/\eta^{\mathrm{ACS}} \tag{9}$$

$$0 \leqslant P_{c,n,t}^{\mathrm{IDC\text{-}ACS}} \leqslant P_{c}^{\mathrm{ACS\text{-}R}} \tag{10}$$

where $\mathrm{H_{c,n,t}^{SIDC\text{-}ACS}}$ represents the cooling power of the SIDC, η^{ACS} is the coefficient of performance of the air conditioning equipment, and $\mathrm{P_c^{ACS\text{-}R}}$ denotes the capacity of the air conditioning units allocated to the DC.

2.2 IDC data demand characteristics

In this study, based on our research, it is believed that the data workload tasks received by the SIDC from agent a owned by Internet service companies (ISCs) c during period t ($W_{\mathrm{Lc},a,t}^{0}$) follow a truncated Gaussian distribution [19], mathematically expressed as

$$f\left(W_{\mathrm{Lc},a,t}^{0}\right) = 1/\sqrt{2\pi}\sigma_{a,t} \exp\left[-\left(W_{\mathrm{Lc},a,t}^{0} - \bar{W}_{\mathrm{Lc},a,t}\right)^2/2(\sigma_{a,t})^2\right] \tag{11}$$

$$0 \leqslant W_{\mathrm{Lc},a,t}^{0} \leqslant W_{\mathrm{Lc},a,t}^{\max} \tag{12}$$

where $\bar{W}_{\mathrm{Lc},a,t}$ is the mean value of the data workload demand from agent a during period t; $\sigma_{\mathrm{a,t}}$ represents the standard deviation of the data workload demand from agent a during period t; and $W_{\mathrm{Lc},a,t}^{\max}$ signifies the maximum predicted data workload demand from agent a at time t. Thus, the initial total data workload of the SIDC at time t before participating in the DR can be denoted as

$$W_{\mathrm{Lc},t}^{0} = \sum_{n\in\Omega^N} W_{\mathrm{Lc},a,t}^{0} \tag{13}$$

2.3 Data load characteristics

In this section, we use an aggregated VPG model along with an ASIDC load model to accurately represent aggregated data networks [6], which includes two steps. In step 1, a VPG is proposed to model a data network [20]. In step 2, a framework with an aggregated virtual generator and aggregated virtual load is proposed to model the aggregated VPG. We used the geographical load balancing (GLB) method to allocate the SIDC workloads. The derivation process of the following equations is provided in detail in [20].

In the VPG, for all SIDCs of an agent, the initial energy planning is regarded as a virtual load, and a virtual generator represents the load regulation potentials, which together replace all the nonelectrical components [20]. Eq. (14) is the potential for spatial load shifting demonstrated by the GLB method, where the initial term represents the baseline power consumption of the SIDC, and the latter portion is the adjusted load of the SIDC. Eq. (15) is a workload balance constraint, which means that the total adjusted workload of all SIDCs is equal to zero and is equal to (18). Eq. (16) expresses the maximum load regulation potential. Eq. (17) shows the limitations of the limited computing resources when performing load transfer.

$$O_{\mathrm{Vc},n,t}^{\boldsymbol{SIDC}} = P_{c,n,t}^{\boldsymbol{SIDC-base}} - D_{\mathrm{Vc},n,t}^{\boldsymbol{SIDC-ad}} \tag{14}$$

$$\sum_{n=1}^{N_{\mathrm{umc}}^{N}} \left(D_{\mathrm{Vc},n,t}^{\boldsymbol{SIDC-ad}}/a_{c,n,t}^{\boldsymbol{SIDC}}\right) = 0 \tag{15}$$

$$D_{\mathrm{Vc},n,t}^{\boldsymbol{SIDC-ad}} \leqslant P_{c,n,t}^{\boldsymbol{SIDC-inc}} \tag{16}$$

$$-D_{\mathrm{Vc},n,t}^{\boldsymbol{SIDC-ad}} \leqslant P_{c,n,t}^{\boldsymbol{SIDC-inc-na}} \tag{17}$$

$$\sum_{n=1}^{N_{\mathrm{umc}}^{N}} \left(P_{c,n,t}^{\boldsymbol{SIDC-base}}/a_{c,n,t}^{\boldsymbol{SIDC}}\right) = \sum_{n=1}^{N_{\mathrm{umc}}^{A}} W_{\mathrm{Lc},a,t} \tag{18}$$

where c, a, and n are the subscript indices for the ISCs, agents, and IDCs owned by an agent, respectively. Num_c^N and Num_c^A are the number of IDCs and agents belonging to the ISC c. $O_{\mathrm{V}}^{\boldsymbol{SIDC}}$ is the power consumption baseline of an SIDC, $P^{\boldsymbol{SIDC-base}}$ is the power consumption baseline of the SIDC, $D_{\mathrm{V}}^{\boldsymbol{SIDC-ad}}$ is the adjusted SIDC power consumption compared with the baseline, $a^{\boldsymbol{SIDC}}$ is the increased power consumption in the SIDC when a unit amount of workload is processed,$P^{\boldsymbol{SIDC-inc}}$ is the increased power computation of the SIDC when a baseline amount of workload is processed, and $P^{\boldsymbol{SIDC-inc-na}}$ is the increased power computation of the SIDC when non-active servers process the maximum workload.

$$\alpha_{c,n,t}^{\boldsymbol{SIDC}} = \left(1+\varpi_1^{\boldsymbol{cool}}\right) \frac{\left(N_{\mathrm{umc},n}^{\boldsymbol{E}} P_{c,n}^{\boldsymbol{E-N}} + N_{\mathrm{umc},n}^{\boldsymbol{A}} P_{c,n}^{\boldsymbol{A-N}} + N_{\mathrm{umc},n}^{\boldsymbol{C}} P_{c,n}^{\boldsymbol{C-N}}\right)/Num_{c,n}^{\boldsymbol{Ser}}}{\left(\bar{\gamma}_{c,n} - 1/t^{t-d}\right) + \left(P_{c,n,t}^{\boldsymbol{Ser-max}} - P_{c,n,t}^{\boldsymbol{Ser-min}}\right)/\bar{\gamma}_{c,n}} \tag{19}$$

$$P_{\mathrm{c,n,t}}^{\boldsymbol{SIDC-base}} = D_{\mathrm{Vc,n,t}}^{\boldsymbol{SIDC-ad}} + \frac{\varpi_1^{\boldsymbol{cool}} \Delta T_{\mathrm{emc},n,t}}{R_{c,n}^{\boldsymbol{eq-th}}} + \left(1+\varpi_1^{\boldsymbol{cool}}\right) P_{c,n,t}^{\boldsymbol{o-e}} + \varpi_2^{\boldsymbol{cool}} \tag{20}$$

$$P_{\mathrm{c,n,t}}^{\boldsymbol{SIDC-inc}} = D_{\mathrm{Vc,n,t}}^{\boldsymbol{SIDC-ad}} \tag{21}$$

$$P_{\mathrm{c,n,t}}^{\boldsymbol{SIDC-inc-na}} = \alpha_{\mathrm{c,n,t}}^{\boldsymbol{SIDC}} \left(\bar{\gamma}_{c,n} - \frac{1}{t^{t-d}}\right) N_{\mathrm{um},c,n}^{\boldsymbol{Ser}} - D_{\mathrm{Vc,n,t}}^{\boldsymbol{SIDC-ad}} \tag{22}$$

where $\varpi^{\boldsymbol{cool}}$ is an empirical constant for the SIDC cooling system. $N_{\mathrm{umc},n}^{\boldsymbol{E}}$,$N_{\mathrm{umc},n}^{\boldsymbol{A}}$, $N_{\mathrm{umc},n}^{\boldsymbol{C}}$, and $N_{\mathrm{umc},n}^{\boldsymbol{Ser}}$ are the numbers of edges, aggregates, core switches, and servers in the SIDC, respectively. $P_{c,n}^{\boldsymbol{E-N}}$, $P_{c,n}^{\boldsymbol{E-N}}$, and $P_{c,n}^{\boldsymbol{E-N}}$ are the rated power consumption of each active edge, aggregate, and core switch, respectively. $\bar{\gamma}_{c,n}$ is the average service rate of the servers, t^{t-d} is the tolerant service delay of the workload, and $P_{c,n,t}^{\boldsymbol{Ser-max}}$ and $P_{c,n,t}^{\boldsymbol{Ser-min}}$ are the peak and minimum power consumption of each active server. $R_{c,n}^{\boldsymbol{eq-th}}$ is the equivalent thermal resistance of the SIDC and $P_{c,n,t}^{\boldsymbol{o-e}}$ is the power consumption of the other equipment.

The workload regulation of all SIDCs from many ISCs constitutes an aggregated virtual generator, whereas their initial energy planning constitutes an aggregated virtual load [6]. The aggregated energy demands and load regulation potentials are given by (23) and (24):

$$O_{\mathrm{V}m,t}^{\boldsymbol{ASIDC}} = \sum_{c=1}^{N_{\mathrm{umc}}} \sum_{n=1}^{N_{\mathrm{umc}}^N} b_{m,c,n,t} O_{\mathrm{Vc,n,t}}^{\boldsymbol{SIDC}} \tag{23}$$

$$D_{\mathrm{V}m,t}^{\boldsymbol{ASIDC}} = \sum_{c=1}^{N_{\mathrm{umc}}} \sum_{n=1}^{N_{\mathrm{umc}}^N} b_{m,c,n,t} D_{\mathrm{Vc,n,t}}^{\boldsymbol{SIDC}} \tag{24}$$

where m is the subscript index for ASIDCs and b is the incidence status (0 or l).

Furthermore, the aggregated VPG-based ASIDC load model is represented in Eqs. (25)–(28). Its parameters are given by Eqs. (29)–(32). $O_{\mathrm{V}m,t}^{\boldsymbol{ASIDC}}$ is the output variable, an $D_{\mathrm{V}m,t}^{\boldsymbol{ASIDC}}$ is the decision variable.

$$O_{\mathrm{V}m,t}^{\boldsymbol{ASIDC}} = P_{m,t}^{\boldsymbol{ASIDC-base}} - D_{\mathrm{V}m,t}^{\boldsymbol{ASIDC-ad}} \tag{25}$$

$$\sum_{m=1}^{N_{\mathrm{umc}}^M} \left(D_{\mathrm{V}m,t}^{\boldsymbol{ASIDC-ad}} / a_{m,t}^{\boldsymbol{ASIDC}}\right) = 0 \tag{26}$$

$$D_{\mathrm{V}m,t}^{\boldsymbol{ASIDC-ad}} \leqslant P_{m,t}^{\boldsymbol{ASIDC-inc}} \tag{27}$$

$$-D_{\mathrm{V}m,t}^{\boldsymbol{ASIDC-ad}} \leqslant P_{m,t}^{\boldsymbol{ASIDC-inc-na}} \tag{28}$$

$$a_{m,t}^{\boldsymbol{ASIDC}} = \max\left(b_{m,c,n,t} a_{c,n,t}^{\boldsymbol{SIDC}}\right) \tag{29}$$

$$P_{m,t}^{\boldsymbol{ASIDC-base}} = \sum_{c=1}^{N_{\mathrm{umc}}} \sum_{n=1}^{N_{\mathrm{umc}}^N} b_{m,c,n,t} P_{c,n,t}^{\boldsymbol{SIDC-base}} \tag{30}$$

$$P_{m,t}^{\boldsymbol{ASIDC-inc}} = \sum_{c=1}^{N_{\mathrm{umc}}} \sum_{n=1}^{N_{\mathrm{umc}}^N} b_{m,c,n,t} P_{c,n,t}^{\boldsymbol{SIDC-inc}} \tag{31}$$

$$P_{m,t}^{\boldsymbol{ASIDC-inc-na}} = \sum_{c=1}^{N_{\mathrm{umc}}} \sum_{n=1}^{N_{\mathrm{umc}}^N} b_{m,c,n,t} P_{c,n,t}^{\boldsymbol{SIDC-inc-na}} \tag{32}$$

Eq. (25) is the potential for the spatial load shifting demonstrated by the GLB method, where the initial element represents the baseline of power usage of the ASIDC, and the subsequent section denotes the modified cumulative load of the SIDC. Eq. (26). is a workload balance constraint that represents the essence of the spatial coupling of the ASIDCs. Eq. (27) expresses the maximum load regulation potential. Eq. (28) shows the issue of limited computing resources when performing load transfer. Eqs. (29)–(32) are used to calculate these parameters.

2.4 Uncertainty modeling based on Z-number method

To effectively account for the influence of the willingness of the end-user supplying data to the SIDC, this study defines the "engagement factor γ" and incorporates it into Eqs. (32) and (33) to obtain the SIDCs total data load model adjusted for user engagement. Mathematically:

$$\sum_{t}^{T} W_{\mathrm{Lc},a,t} = \sum_{t}^{T} W_{\mathrm{Lc},a,t}^{0} \tag{33}$$

$$\left(W_{\mathrm{Lc},a,t}^{0} - W_{\mathrm{Lc},a,t}^{\boldsymbol{ava}} \leqslant W_{\mathrm{Lc},a,t}^{\mathrm{act}} \leqslant W_{\mathrm{Lc},a,t}^{0}\right. \tag{34}$$

$$W_{\mathrm{Lc},a,t}^{\boldsymbol{ava}} = \gamma_{c,a,t}^{\boldsymbol{DR}} W_{\mathrm{Lc},a,t}^{0} \tag{35}$$

where $W_{\mathrm{Lc},a,t}^{\mathrm{act}}$ represents the load capacities in SIDC-DR at time period t; $W_{\mathrm{Lc},a,t}^{\boldsymbol{ava}}$ is the data load amounts adjusted based on user willingness participation; $\gamma_{\mathrm{c,a,t}}^{\mathrm{DR}}$ is the participation willingness workload factor, which value is between [0,1]. The higher the γ value, the greater the willingness of the SIDC-DR. When γ equals 1, it implies that the actual available capacity of the SIDC-DR is equivalent to its technical theoretical value.

Influenced by behavioral habits and cognitive abilities, end users providing data to SIDCs have a high degree of specificity regarding their sensitivity to incentive pricing [19]. To illustrate the connection between the incentive price and willingness factor, this study introduces a price

elasticity coefficient. This coefficient represents the sensitivity of end users providing data to SIDCs in time segment t concerning their willingness to engage in SIDC-DR owing to changes in the incentive price. The detailed formula is as follows:

$$\gamma_t = \gamma_t^0 \left[\varepsilon_t \left(\pi_t^{dch} - \pi_t^0\right)\right] / \pi_t^0 \tag{36}$$

where π_t^{dch} signifies the reward price given by the grid to SIDC users for the duration of time segment t. π_t^0 represents the benchmark incentive price. γ^0 indicates the baseline willingness level of end users to participate in DR under the benchmark incentive price.

The uncertainty of user willingness to participate in DR is part of the uncertainty in the cognitive process. The reliability of the data itself is also an indispensable factor affecting the model built in this study; that is, the uncertainty of the cognitive results should also be taken into consideration.

In summary, because the high specificity of users' sensitivity to incentive prices and the credibility of information should be considered, this research incorporates the Z-number approach to represent the uncertainty in the price elasticity coefficient ε_t [22]. The Z-number theory proposes the use of a binary ordered fuzzy number $(\widetilde{\mathrm{M}}, \widetilde{\mathrm{N}})$ to describe the effect of uncertain variables x (in this study, it refers to the price elasticity coefficient ε_t) [23]. Without loss of generality, this study assumes that the uncertainty distribution of the user's price elasticity coefficient ε_t and its information credibility follows a trapezoidal distribution and a triangular distribution, respectively [21].

The steps of the entire process are shown below:

a) For the Z-number parameter $\mathrm{Z}(\varepsilon) = \left(\widetilde{\mathrm{M}}, \widetilde{\mathrm{N}}\right)$, the first step is to defuzzify the information confidence level $\widetilde{\mathrm{N}}$ and convert it into a definite number α_{N}.

$$\alpha_N = \int x o_{\widetilde{N}}(x)\mathrm{d}x \Big/ \int o_{\widetilde{N}}(x)\mathrm{d}x \tag{37}$$

b) The result of the definite number α_{N} is input into (38) in the form of a weight, calculating the α-cut $o_{\widetilde{\mathrm{M}}^{\alpha}}(\mathrm{x})$ of the Z-number. The processing results are shown in Fig. 2.

$$o_{\widetilde{M}^{\alpha}}(x) = \alpha_N o_{\widetilde{M}}(x) \tag{38}$$

c) To further obtain the standard fuzzy set $\widetilde{Z}'$, the Z-number with weight constraints is processed according to (39). The results are shown in Fig. 3.

$$\widetilde{Z}' \to o_{\widetilde{Z}'}(x) = o_{\widetilde{M}}\left(x/\sqrt{\alpha}\right) \tag{39}$$

d) Using the centroid method, $o_{\widetilde{Z}'}(\mathrm{x})$ is converted into a probabilistic transformation, ultimately determining its equivalent probability distribution $\mathrm{f}(\mathrm{x})$.

$$f(x) = o_{\widetilde{Z}'}(x) \Big/ \int_0^{+\infty} o_{\widetilde{Z}'}(x)\mathrm{d}x \tag{40}$$

The aforementioned treatment converts the Z-number parameters (price elasticity coefficient ε_t) in the ASIDCs participating in DR (ASIDC-DR) model into an equivalent probabilistic form, and γ under a specific incentive price is ultimately known. The relevant results are input into Eqs. (37)–(39) to obtain the ASIDC-DR capacity model, considering the impact of user participation willingness.

3 IDC-DR Capacity Value Assessment

3.1 Optimized dispatch of power systems considering ASIDC-DR

This study establishes an optimization dispatch model for a power system with an ASIDC under fault conditions using the sum of the system power shortage costs and the costs paid to the ASIDC for DR as the objective function, as follows:

$$\min V = \omega_1 \bar{C}^{\mathrm{usd}} + \omega_2 \bar{C}^{\mathrm{dr}} \tag{41}$$

$\bar{C}^{\mathrm{usd}}$ and $\bar{C}^{\mathrm{dr}}$ represent the system power outage cost and DR fee paid to the ASIDC, respectively. ω_1 and ω_2 are weighting coefficients, and $\omega_1 + \omega_2 = 1$.

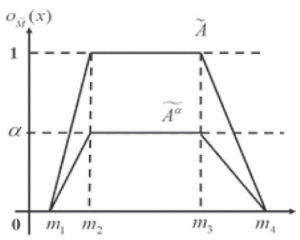

Fig. 2. α-cut of the Z-number parameters.

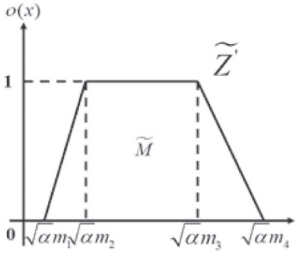

Fig. 3. Normalization of Z-number parameters.

$$\bar{C}^{usd} = \sum_{t}^{T} \psi_t^{usd} P_t^{usd} \tag{42}$$

$$\bar{C}^{dr} = \psi_t^{dr} \sqrt{\sum_{t}^{T} \left(O_{Vm,t}^{AIDC} - P_{m,t}^{AIDC-base} \right)^2} \tag{43}$$

Eqs. (45) and (46) define the costs involved in power outages and DR incentives. Among them, ψ_t^{usd} and ψ_t^{dr} respectively represent the cost of power grid load shedding and the DR incentive price paid. P_t^{usd} represents the total load shedding power of the system at each time interval t, where ψ_i^{usd} is the load loss value of the node.

Essentially, these equations strive to balance the economic impacts of power outages with the costs of DR incentives, thereby minimizing the total system cost while ensuring reliability. The weighting coefficients ω_1 and ω_2 allow the model to adjust the emphasis on load-shedding costs versus DR costs based on the specific requirements and objectives of the power system.

The SIDCs' dispatch optimization must satisfy the following constraints: Eq. (44) represents the traditional equation constraint for the node power balance. Constraints (45)–(47) were employed to simulate the active power flow in a power system that integrates SIDCs. To ensure the system safety, (48) and (49) limit the node voltage deviation and line load flow, respectively.

$$\sum_{i\in\Omega_I} P_{i,t}^{dg} + \sum_{(i,j)\in\Omega_F} \left(P_{ij,t}^{fm} - P_{ij,t}^{to} \right) = \sum_{m\in\Omega_M} P_{n,t}^{SIDC} + \sum_{i\in\Omega_I} P_{i,t}^{user}, \forall t \in T \tag{44}$$

$$P_{ij,t}^{fm} + P_{ij,t}^{to} = R_{ij} I_{ij,t}^2 \quad \forall (i,j) \in \Omega_F, \forall t \in T \tag{45}$$

$$P_{ij,t}^{fm} - P_{ij,t}^{to} = \frac{R_{ij}\left(V_{i,t}^2 - V_{j,t}^2 \right)}{Z_{i,j}^2}, \forall (i,j) \in \Omega_F, \forall t \in T \tag{46}$$

$$I_{ij,t} = \left(V_{i,t} - V_{j,t} \right) / Z_{ij} \quad \forall (i,j) \in \Omega_F, \forall t \in T \tag{47}$$

$$V_{k,\min} \leqslant V_{k,t} \leqslant V_{k,\max} \quad \forall k \in \Omega_D, \forall t \in T \tag{48}$$

$$0 \leqslant I_{ij,t} \leqslant I_{ij,\max} \quad \forall (i,j) \in \Omega_F, \forall t \in T \tag{49}$$

In addition, the optimization process must satisfy the ASIDC operational characteristic constraints, as described in Section "IDC-DR capacity value assessment".

The main decision variables in the optimization model include P_t^{usd}, $O_{Vm,t}^{ASIDC}$, along with the control and state variables pertinent to the operations of the ASIDC.

To determine the CV based on SIDC-DR, it is necessary to analyze and compare the reliability levels of scenarios with and without SIDC-DR.

3.2 Iterative process

To achieve this goal, this study employed the SMCS method. Considering the modeling of the system components and the CV assessment metrics previously addressed, Fig. 4. outlines the detailed procedure for computing the CV index using SIDC-DR.

The detailed process is as follows:

Step 1) Establish a chronological sequence of power generation and load demands for the system $\{P_t^{ASIDC\text{-}base}\}$.

Step 2) Assess system reliability metrics without/with SIDC-DR($EENS^{base}$/ $EENS^{DR}$).

2-1-1) Calculate the power output of all generator units.

2-1-2) Calculate the total power load without SIDC-DR.

$\sum_{All\ power\ load} P_t^{d0}$. That is:

$$P_t^{d0} = P_t^{user} + P_t^{ASIDC\text{-}base}$$

2-1-3) Compare the power output of all generator units with $\sum_{All\ power\ load} P_t^{d0}$ to establish whether there is a load

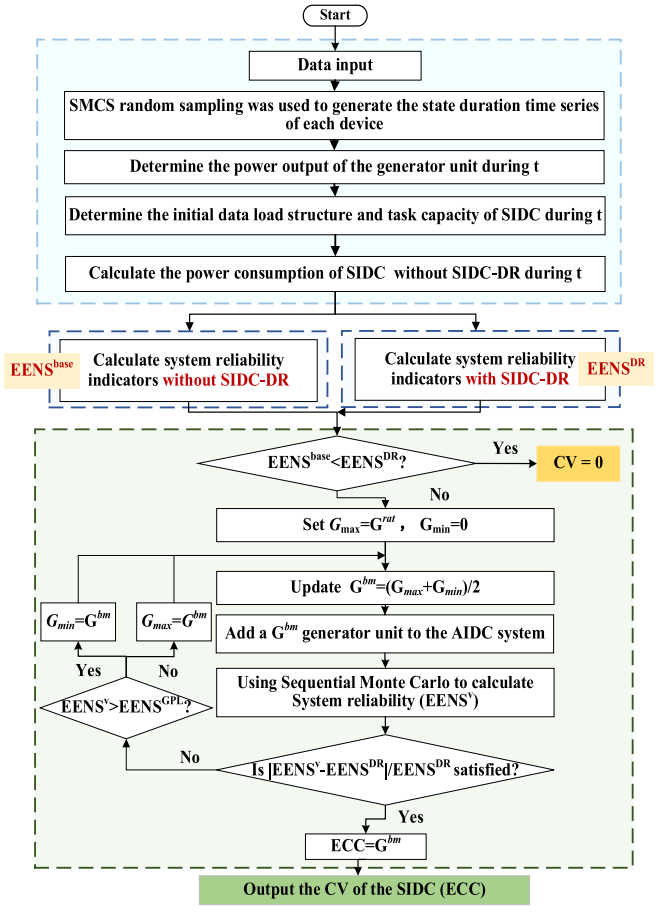

Fig. 4. CV calculation process based on SIDC-DR.

loss during t; that is, determine whether there is $(\sum_{\text{All power load}} P_t^{d0} > \sum_{\text{All generator units}} P_t^{dg})$.

2-1-4) In the event of load loss, the system load loss for time period t is computed based on formula 2-1-2), and further calculate E_{ENS}^{base} according to (3).

$$P_t^{usd0} = \sum_{\text{All power load}} P_t^{d0} - \sum_{\text{All generator units}} P_t^{dg}$$

2-1-5) For each time period t, repeat Steps 2-3) to 2-4) until the end of the current simulation year.

2-1-6) The reliability index results of the system without SIDC-DR were calculated and determined according to Formula (2), that is E_{ENS}^{base}.

2-1-7) Repeat Steps 2-1) to 2-6) until $\frac{\sigma(E_{ENS}^{base})}{\sqrt{N}\times E(E_{ENS}^{base})} \leqslant 0.05$ is met, where, N is the number of simulation years, and $E(E_{ENS}^{base})$ and $\sigma(E(E_{ENS}^{base}))$ represent the expectation and standard deviation of the corresponding E_{ENS} value in the simulation years, respectively.

2-1-8) Output the results $E(E_{ENS}^{base})$ as the benchmark, which is the reliability index of the system without SIDC-DR.

2-2-1) In line with 2-1-1).

2-2-2) Determine the ASIDC willingness coefficient γ using the SMCS method.

2-2-3) Determine the capacity of the ASIDC load that can be used for SIDC-DR after considering the influence of user participation intention.

2-2-4) Calculate $\sum_{\text{All power load}} P_t^d$; the specific calculation formula is as follows:

$$P_t^d = P_t^{user} + O_{vt}^{ASIDC\text{-}base}$$

2-2-5) In line with 2-1-3).

2-2-6) If load loss occurs, the load C_Vs from Steps 3-3) are considered as established parameters (specifically, as boundary conditions). The scheduling cycle is then set to the '24 h' of the day associated with the fault period t. By solving the "scheduling optimization model of the power system with SIDC-DR under the fault state" described in Section "System data", the system load loss value corresponding to this period t can be obtained, and ENS_t^{DR} can be further obtained.

2-2-7) Repeat Steps 2-2-5) to 2-2-6) until the end of the current simulation year.

2-2-8) Calculate E_{ENS}^{DR}.

2-2-9) Repeat Steps 2-2-1) to 2-2-8) until $\frac{\sigma(E_{ENS}^{DR})}{\sqrt{N}\times E(E_{ENS}^{DR})} \leqslant 0.05$ is met.

2-2-10) Record the result in this scenario as E_{ENS}^{DR}. It is the system reliability index when accounting for ASIDC-DR.

The specific calculation process is shown in Fig. 5.

Step 3) CV calculation

Comparison of E_{ENS}^{base} and E_{ENS}^{DR}. If $E_{ENS}^{base} < E_{ENS}^{DR}$, set the CV of ASIDC-DR to 0; otherwise, perform the following steps.

3-1) Define two auxiliary variables G_{max} and G_{min}, and let $G_{max} = G^{rat}$, $G_{min} = 0$, where G^{rat} is a positive real number given artificially.

3-2) In the scenario without SIDC-DR, it is assumed that a virtual benchmark generator unit is added at the ASIDC grid-connected location with a configured capacity of $G^{bm} = (G_{max} + G_{min})/2$, and the FOR is set to 0.08 %.

3-3) The SMCS method is used to evaluate the E_{ENS} index and record it as E_{ENS}^{v}.

3-4) Compare E_{ENS}^{v} with E_{ENS}^{DR} values, and adjust the configured capacity of the virtual reference generator unit accordingly. Specifically, if $E_{ENS}^{v} > E_{ENS}^{DR}$, then let $G_{min} = G^{bm}$, and G_{max} keep its value in the last iteration; otherwise, let $G_{max} = G^{bm}$, and leave the value of G_{min} unchanged.

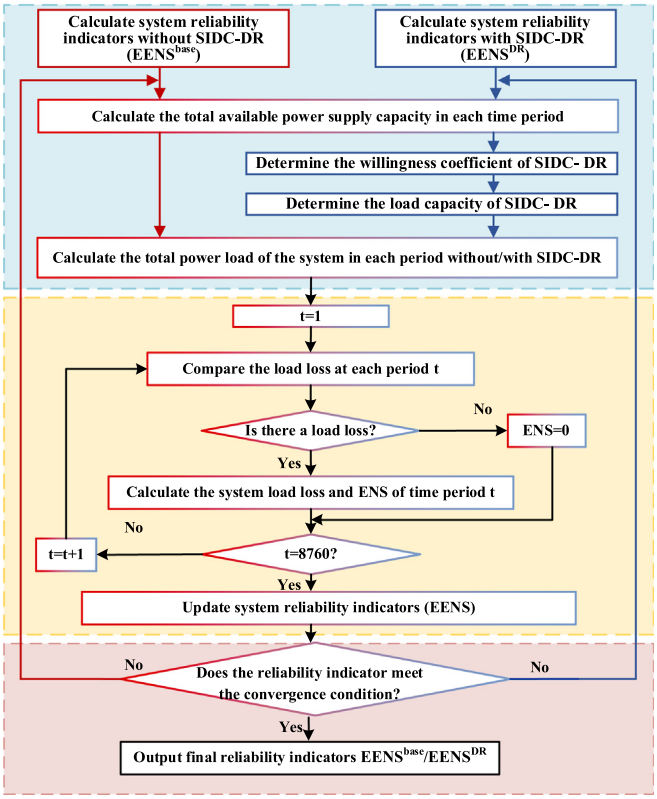

Fig. 5. Calculation process for system reliability indicators with/without SIDC-DR.

3-5) Update the result of G^{bm} as $G^{bm} = (G_{max} + G_{min}) / 2$, and calculate the system E_{ENS} value (E^{v}_{ENS}) after adjusting the generation capacity again.

$$\frac{|E^{N}_{ENS} - E^{DR}_{ENS}|}{(E^{DR}_{ENS})} \leqslant \zeta \tag{50}$$

3-6) Check whether Eq. (50) is satisfied ($\zeta = 1\%$ in this paper); if so, identify the obtained result G^{bm} as ECC value based on ASIDC-DR and go to Step 5); otherwise, return to Step 3-1) and continue.

Step 4) Output the ECC result as the final CV value.

4 Case analysis

4.1 System data

To verify the effectiveness of the proposed model and method, we selected an improved IEEE-33 node network as an example for simulation validation. There are two ISCs, both of which have four SIDCs. The three SIDCs owned by ISC1 are at Bus2, Bus5, and Bus21, whereas the three SIDCs owned by ISC2 are at Bus31, Bus27, and Bus13. The total load was 4560 MW, where the effective SIDC load was set to 50 % of the maximum computing workload, and the additional load changes were distributed among the other loads in proportion to their original values. The proportion of the SIDC load was 9.6 %.

The generation costs were the same as those in [24] and the generation costs for the renewable energy sources were 0.

Data Network 1 had two agents and five data lines, whereas Data Network 2 had two agents and four data lines.

$$W_{L1,1,t} = W_{L1,2,t} = W_{L2,1,t} = W_{L2,2,t} = 0.5 \times 10^{7}\text{request/s}$$

The structures of the data networks and the IEEE-33 node network are shown in Fig. 6.

In this system, there were a total of 32 feeder lines and 33 load nodes. It was connected to an external grid through a distribution substation that served as a balancing node. In this scenario, the wind turbine unit is situated at node 11, and the conventional gas turbine unit is situated at node 15, boasting a 3 MW installation capacity. Relying on past statistical records, the reliability metrics are defined with a mean time to failure (MTTF) of 1300 h and a mean time to repair (MTTR) of 50 h. The users have an annual peak load demand of 13.6 MW. The highest yearly load data for each node aligned with those of the IEEE 33-node distribution system. The conventional generation unit model, wind turbine model, and parameters used in this study were derived from [15]. The energy storage unit and load models, along with their parameters, were obtained from [16] and [17], respectively. The parameter settings in this article are as follows, with some parameters referenced from [25] (see Table 1).

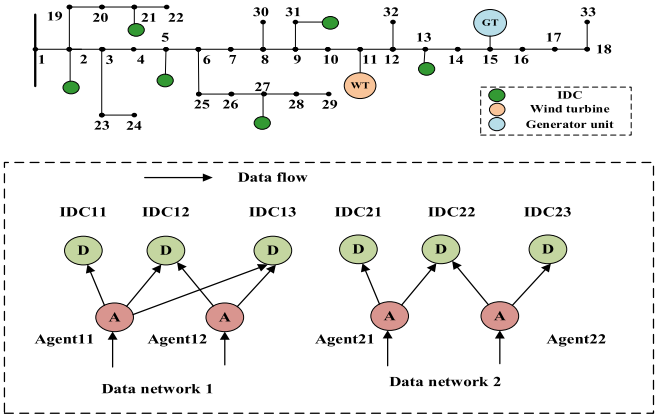

Fig. 6. Improved IEEE-33 node network and data network structure.

4.2 Simulation results

This case study initially focused on simulating and verifying the dispatch outcomes of the electrical grid associated with the ASIDC involvement in DR, both before and after engagement. To this end, we delineated two principal scenarios.

Scenario One: The ASIDC does not participate in DR.
Scenario Two: The ASIDC engages in grid-side DR.

Fig. 7 presents the actual output of wind turbines under two scenarios. It is evident from the figure that in the absence of ASIDC participation in the DR, there is a suboptimal match between the wind turbine output and load demand, leading to wind energy curtailment in certain periods, adversely impacting the economic benefits of the system. However, with the incorporation of the ASIDC flexibility, the utilization rate of RES significantly improves, which also demonstrates that the model effec-

Table 1
Simulation system SIDC parameters.

Parameters	Values	Parameters	Values
η^{DC}	0.9	$\bar{\gamma}_{c,n}$	20 request/s
ϖ_1^{cool}	0.5	$t^{t\text{-}d}$	0.1 s
ϖ_2^{cool}	1.25 MW	$\Delta T_{emc,n}$	3 °C
$R^{eq-th}_{c,n}$	0.1 ¥/Gbps	$P^{Ser-max}_{c,n}$	0.2×10^{-3} MW
$P^{Ser-min}_{c,n}$	0.1×10^{-3} MW	$P^{o-e}_{c,n}$	1.25 MW
$P^{E-N}_{c,n}/P^{A-N}_{c,n}/P^{C-N}_{c,n}$		$0.19/0.18/0.24 \times 10^{-3}$ MW	
$N^{E}_{umc,n}/N^{A}_{umc,n}/N^{C}_{umc,n}/N^{Ser}_{umc,n}$		75,000/2500/1250/5000	

tively balances the economic and environmental benefits. As shown in Fig. 8, integrating the ESS with SIDC effectively enhanced the RES absorption rate. In addition, ESS discharging during peak periods increases the reliability of SIDC services, confirming the effectiveness of ESS integration.

Fig. 9 and Fig. 10 display data for two SIDCs in each scenario, showing the 24-hour operation of the servers and the corresponding total energy consumption of the ASIDC. A comparison between Fig. 9 and Fig. 10 clearly reveals that participating in the DR improves the server utilization in SIDCs and optimizes the energy consumption curve. Fig. 11 presents the data load demand curve and power purchasing profiles of the remaining two SIDCs, highlighting significant changes in data demand during peak periods before and after participating in the DR. This underscores the effectiveness of the DR in guiding SIDCs to allocate their data demands, thereby reducing external power purchasing costs.

The proportion of various data loads in a data center directly affects the available virtual generation capacity of the entire SIDC-DR. Therefore, we focus on the DR rate (γ) in data load characteristics. It is defined as the ratio of the load that can participate in the DR to the total information load. Based on practical situations, this value varies between 0 and 50 %. This study tested the CVs of data centers participating in DR under different incentive price settings. Incentive prices were set for the stair-step segments, as listed in Table 2.

The calculated CVs are shown in Fig. 12.

Analyzing the results from Fig. 12, in all four scenarios, the CV increases with the increase in the DR rate (γ) and tends to saturate after the DR rate reaches a certain threshold. This outcome confirms that the adjustability of the data load is a fundamental factor affecting the confidence in the CV of the SIDC. The figure also shows that the CV is closely related to the participation level of the end users. Under the same DR rate (γ) conditions, the CV estimated value for Scenario 4 with the highest incentive price is the highest, while the CV estimated value for

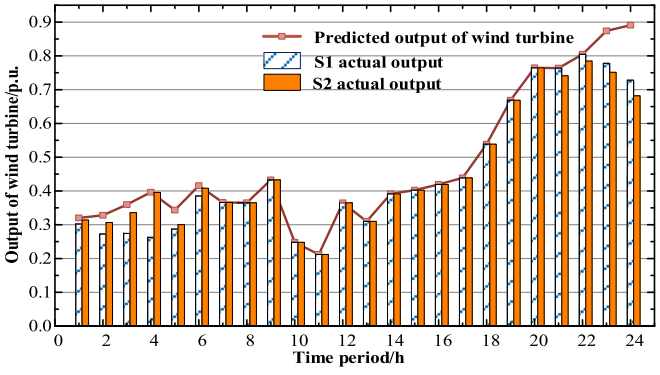

Fig. 7. Output of wind turbines under two scenarios.

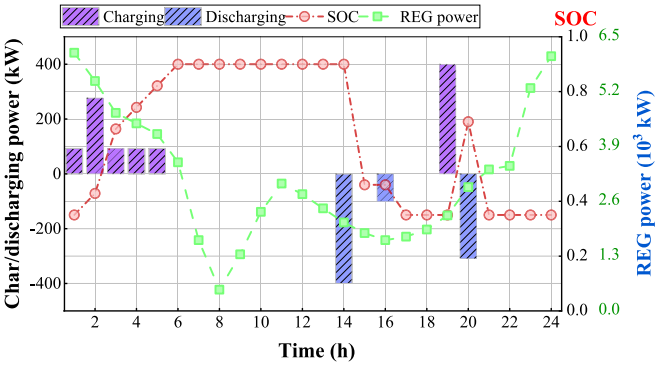

Fig. 8. ESS charging and discharging status and the RES output.

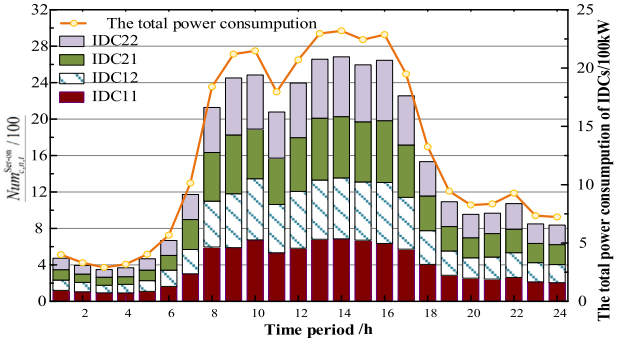

Fig. 9. Number of active servers and the total energy consumption of SIDCs of Scenario One.

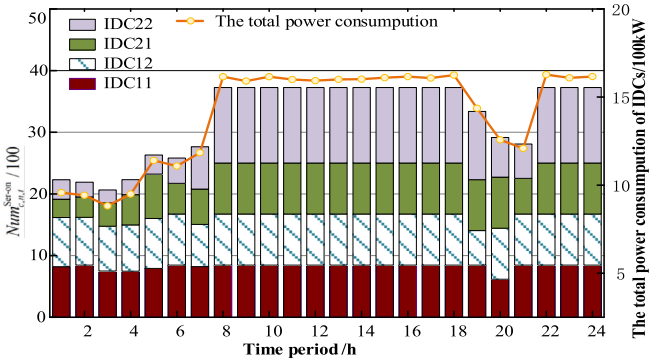

Fig. 10. Number of active servers and the total energy consumption of SIDCs of Scenario Two.

Scenario 1 with the lowest incentive price is the lowest, which means that the higher the incentive, the stronger the willingness of users to participate in the DR program, which will accordingly bring greater capacity benefits for the implementation of DR. Furthermore, the results in Fig. 12 also show that the EENS decreases with increases in incentive pricing and DR rate, demonstrating that SIDC-DR enhances system reliability.

In an actual market environment, the willingness of different individual users to participate in the DR program at

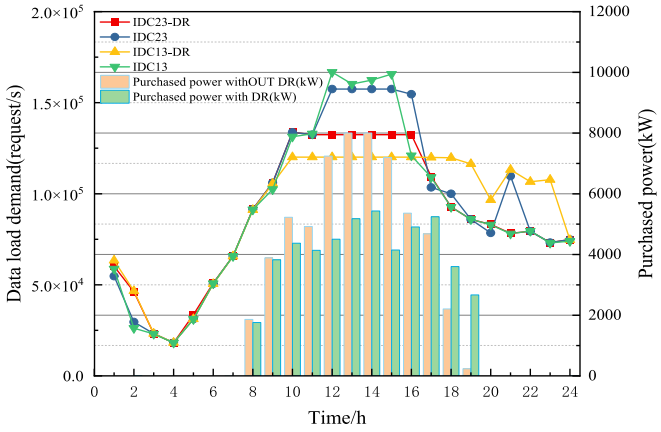

Fig. 11. Data load demand and SIDC power purchasing capacity.

Table 2
Incentive price setting.

Scenario	#1	#2	#3	#4
Incentive price (CNY/kWh)	0	0.6	1.2	1.8

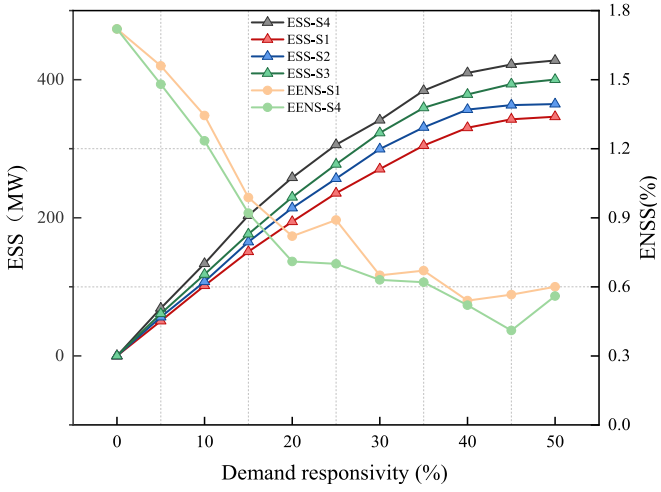

Fig. 12. CVs under different DR rates.

the same incentive price varies because of differences in user cognition.

In the SIDC-DR operational characteristics model proposed in this study, the effects of the above factors are explicitly considered. This study sets up four scenarios to represent different user sensitivities to the same incentive price, as shown in Table 3.

In Scenario 1, the price elasticity coefficient of SIDC is set to 1, implying that SIDC fully participates in DR. Scenarios 2, 3, and 4 are set with the price elasticity coefficient of SIDC that satisfies the Z-number value, with midpoints of 0.3, 0.6, and 0.9, respectively.

The DR incentive price is set to 2.4 yuan/kWh. The SIDC-DR rate is set at 40 %. Using the CV assessment process presented in this study, the CV of the system under different price elasticity coefficient scenarios was calculated.

Furthermore, considering that there is no definitive conclusion regarding the benefits to the system of artificially increasing the DR CV, this study calculates the utility cost of the system load loss before and after implementing DR, and obtains the cost change in the system load loss caused by implementing DR. Specific calculation involves Eqs. (42) and (43), where ψ_i^{usd} is set in the text as \$2.55/kW.

The calculated results are shown in Fig. 13.

By comparing the results in Fig. 13, it can be observed that when considering the influence of the price elasticity coefficient, there is a significant change in the CV of the SIDC. Specifically, when adopting a fully deterministic model without considering the uncertainty of SIDC participation volition (Scenario 1), all SIDCs participate in the DR, resulting in the highest evaluated CV value. However, the willingness and dynamic changes in SIDC participation in DR are, in reality, uncertain. As the price elasticity coefficient decreases, the derived CV value changes accordingly. In addition, although the consideration of uncertainty in DR implementation increases the costs, as shown in the figure, the system operational costs exhibit a clear downward trend. This indicates that taking into account the load characteristics of SIDCs has a positive impact on the economic efficiency of the system.

A comparative analysis of the simulation results indicates that the willingness of the SIDC-DR and its dynamic changes play a crucial role in determining the CV. Therefore, when establishing the operational characteristics model of the SIDC, the uncertainties in user behavior should be fully considered. Otherwise, decision-makers might idealize the CV of the SIDC, leading to irrational decisions in the expansion planning of smart power systems.

The credibility of the data will significantly influence the CV assessment values. To verify the effectiveness of the established model, this example compares the assessment results of the SIDC CV with different levels of information credibility to determine how neglecting the impact of information credibility affects the CV of data centers.

To this end, under the premise that the demand price elasticity coefficient of the SIDC satisfies the Z-number value with a center point equal to 0.9, four scenarios with different data credibility levels were set:

a) The willingness data of SIDC users participating in DR are fully credible; that is, the impact of data credibility on SIDC modeling is not considered. Thus, in this scenario, the SIDC Z-number model reverts to a traditional fuzzy model.

Table 3
Price elasticity coefficient setting.

Scenario	Information Credibility Level	A Trapezoidal Distribution	B Triangular Distribution	CV Value (kW)
1	–	(0.7,0.8,1.0,1.1)	(1,1,1)	443.94
2	Low	(0.7,0.8,1.0,1.1)	(0.2,0.3,0.4)	308.89
3	Medium	(0.7,0.8,1.0,1.1)	(0.5,0.6,0.7)	365.39
4	High	(0.7,0.8,1.0,1.1)	(0.8,0.9,1.0)	429.86

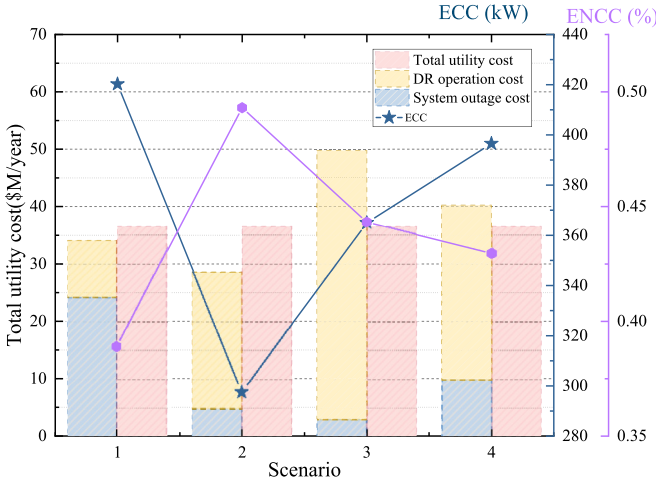

Fig. 13. CV of ASIDC under different elasticity coefficients.

b), c), and d): The credibility of SIDC data concerning users' willingness to participate in DR is low, with the center points of their Z-number model being 0.3, 0.6, and 0.9.

By evaluating the CV of data centers participating in DR for each of the above scenarios, the comparison results illustrate the impact of information credibility on DR assessment. The results are presented in the final column of Table 4.

The results show significant differences in the CV outputs across various scenarios. In real-world engineering projects, there may be various issues related to information distortion in SIDC projects. This leads to biases in the description of SIDC characteristics, thereby affecting the accuracy of the CV assessment. Overlooking these issues significantly diminishes the validity of CV assessment results. Therefore, considering the authenticity of the data is essential for assessing the CV of the SIDC.

In the aforementioned research, this paper set the weight coefficients ω_1 and ω_2 of "reliability benefits" and "economic costs" to equal values. However, in practice, power system operators continuously adjust weight factors based on real-time grid operations. This section focuses on the sensitivity of the dispatch optimization model to the weight coefficients and analyzes the changes in system reliability under different weights. The results shown in Fig. 14 reflect adjustments in ω_1 and ω_2.

It is observed that as ω_2 increases, the $EENS^{DR}$ of the system with SIDC-DR continues to decrease, reaching its minimum when ω_1 and ω_2 are around 0.45 and 0.55 respectively, representing the optimal state of the system. At this point, the system reliability peaks. However, after this point, the index begins to rebound. This indicates that power systems should strategically sacrifice reliability benefits when necessary to ensure the continuous availability of DR in practical applications. If ω_2 is further increased, the economic cost of invoking DR becomes too high, inevitably diminishing the advantages of DR.

The changes in the weight coefficients significantly affect the optimization results. In practical application, the values of ω_1 and ω_2 are assigned based on the specific needs and application scenarios of the operators. By dynamically adjusting these two weights, the system can respond flexibly to different operating conditions and market changes. Employing various scientific methods can more rationally determine the weight coefficients and effectively reduce the impact of subjectivity on the final results. Methods such as

Table 4
Information credibility scenario configuration.

Scenario	Information Credibility Level	A Trapezoidal Distribution	B Triangular Distribution	CV Value(kW)
1	–	(0.7,0.8,1.0,1.1)	(1,1,1)	443.94
2	Low	(0.7,0.8,1.0,1.1)	(0.2,0.3,0.4)	308.89
3	Medium	(0.7,0.8,1.0,1.1)	(0.5,0.6,0.7)	365.39
4	High	(0.7,0.8,1.0,1.1)	(0.8,0.9,1.0)	429.86

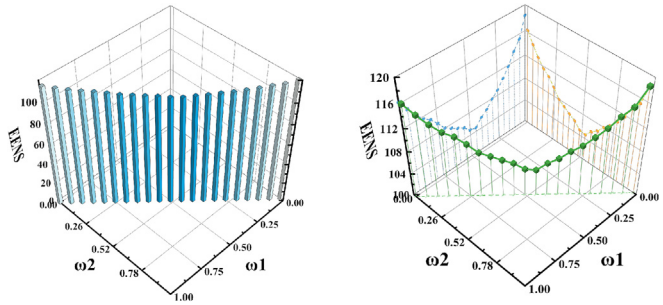

Fig. 14. EENS values under different weight coefficients.

the analytic hierarchy process (AHP), fuzzy comprehensive evaluation, and multi-attribute utility theory are scientific evaluation methods that can be used.

5 Conclusion

This paper introduces a method to evaluate the CV of SIDCs in power systems using ASIDC-DR that focuses on enhancing reliability and economic operation by leveraging SIDC flexibility. The key findings of the simulations are as follows.

1) This study uses ECC to assess CV and EENS as a reliability index. The results show that SIDC participation in DR increases ECC and decreases EENS, demonstrating dual economic and reliability benefits.
2) A detailed model of SIDCs is presented to improve the accuracy of real-time interactive response assessments. The Z-number fuzzy theory is used to model DR volition and address uncertainties in user participation and information credibility. Simulations confirm that incorporating these uncertainties yields predictions that are closer to real-world scenarios.
3) A specific computational procedure based on the ASIDC-DR CV metric is outlined. Simulation results validate the effectiveness of the method in real-world applications.

CRediT authorship contribution statement

Bo Zeng: Resources, Methodology. **Xinzhu Xu:** Writing – review & editing, Writing – original draft. **Fulin Yang:** Writing – review & editing.

Declaration of competing interest

The authors declare that they have no known competing financial interests or personal relationships that could have appeared to influence the work reported in this paper.

Acknowledgments

This work was supported in part by the National Natural Science Foundation of China under Grant 52177082 and in part by the Beijing Nova Program under Grant 20220484007.

References

[1] China's communication service (CCS), China Data Center Industry Development White Paper (2023), distributed by China's communication service (CCS), Dec. 2023, http://www.caict.ac.cn (accessed 20 Feb 2024).
[2] C. Li, K. Zheng, H. Guo, et al., Intra-day optimal power flow considering flexible workload scheduling of IDCs, Energy Rep. 9 (7) (2023) 1149–1159.
[3] X. Chao, C. Gao, D. Li, Mixed operation model of data network and power network and its participation in the economic operation of power system, Proc. CSEE 38 (5) (2018) 1448–1456.
[4] M. Chen, C. Gao, S. Chen, Double-layer economic scheduling model considering the potential of power load regulation in data center, Proc. CSEE 39 (05) (2019) 1301–1314.
[5] M. Chen, C. Gao, M. Shahidehpour, Z. Li, Incentive-compatible demand response for spatially-coupled internet data centers in electricity markets, IEEE Trans. Smart Grid 12 (4) (2021) 3056–3069.
[6] M. Chen, C.W. Gao, M. Shahidehpour, Z. Li, Proliferation of small data networks for aggregated demand response in electricity markets, IEEE Trans. Power Syst. 37 (3) (2022) 2297–2311.
[7] C.J. Dent, A. Hernandez-Ortiz, S.R. Blake, et al., Defining and evaluating the capacity value of distributed generation, IEEE Trans. Power Syst. 30 (5) (2015) 2329–2337.
[8] R.S. Wang, S.L. Wang, G.C. Geng, Q.Y. Jiang, Multi-time-scale credit capacity assessment of renewable and energy storage considering complex operational time series, Appl. Energy (2024), https://doi.org/10.1016/j.apenergy.2023.122382.
[9] S. Jethro, X.J. Jeremiah, F.D. Joseph, An efficient method to estimate renewable energy credit capacity at increasing regional grid penetration levels, Renew. Sustain. Energy Transit. (2022), https://doi.org/10.1016/j.rset.2022.100033.
[10] W. Shi, J. Qu, W. Wang, Wind power operation capacity credit assessment considering energy storage, Glob. Energy Interconnect. 5 (1) (2022) 1–8.
[11] J. Gazijahani, J. Salehi, Reliability constrained two-stage optimization of multiple renewable-based microgrids incorporating critical energy peak pricing demand response program using robust optimization approach, Energy 161 (2018) 999–1015.
[12] B. Zeng, C. Zhang, Quantifying the capacity credit of IDC-based demand response in smart distribution systems, IET Gener. Transm. Distrib. 17 (12) (2023) 2757–2772.
[13] B. Zeng, X. Wei, D. Zhao, et al., Hybrid probabilistic-possibilistic approach for credit capacity evaluation of demand response considering both exogenous and endogenous uncertainties, Appl. Energy 299 (2018) 186–200.
[14] X. Bai, Y. Fan, T. Wang, et al., Dynamic aggregation method of virtual power plants considering the reliability of renewable energy, Electric Power Automat. Equipment 42 (7) (2022) 102–110.
[15] Y. Huang, L. Chen, X. Huang, et al., Performance of natural draft hybrid cooling system of large-scale steam turbine generator unit, Appl. Therm. Eng. 122 (2017) 227–244.
[16] S. Xu, Y. Zhang, Y. Su, Probabilistic power flow calculation in smart distribution networks considering fuzzy correlation between uncertainty variables, Power Syst. Technol. 44 (4) (2020) 1488–1500.

[17] C. Spyridon, N. Athanasios, I. Petros, et al., Smart energy management algorithm for load smoothing and peak shaving based on load forecasting of an island's power system, Appl. Energy 238 (2019) 627–642.
[18] C. Jin, X. Bai, C. Yang, W. Mao, et al., A review of power consumption models of servers in data centers, Appl. Energy (2020).
[19] H. Chen, Z. Li, X. Jin, et al., Modeling and optimization method of active distribution network integrating intelligent buildings, Proc. CSEE 38 (22) (2018) 6550–6563.
[20] M. Chen, C. Gao, Z. Li, et al., Aggregated model of data network for the provision of demand response in generation and transmission expansion planning, IEEE Trans. Smart Grid 12 (1) (2021) 512–523.
[21] B. Zeng, Q. Hu, Y. Liu, et al., Dynamic probabilistic power flow calculation of electric-gas interconnected system considering complex uncertainty of demand response, Proc. CSEE 40 (4) (2020), 1161–1171+1408.
[22] Q. Hu, Dynamic Probabilistic Power Flow Calculation of Electro-Gas Interconnected System Considering Comprehensive Demand Response Uncertainty, Dissertation, North China Electric Power University, 2019.
[23] T. Yao, M. Wu, J. Mao, L. Zhang, A multi-attribute decision-making method based on Z-number spectrum, Stat. Decis. 35 (13) (2019) 44–48.
[24] P.M. Subcommittee, IEEE reliability test system, IEEE Trans Power Apparatus Syst. 98 (6) (1979) 2047–2054.
[25] X. Wei, Credit capacity and Economic Assessment of Electric Vehicle Parking Lots as Virtual Storage Resources. Dissertation, North China Electric Power University, 2020.
[26] D. Wang, C. Xie, R. Wu, et al., Optimal energy scheduling for data center with energy nets including CCHP and demand response, IEEE Access 9 (2021) 6137–6151.
[27] B. Zeng, Y. Zhou, X. Xu, et al., Bi-level planning approach for incorporating the demand-side flexibility of cloud data centers under electricity-carbon markets, Appl. Energy (2024).

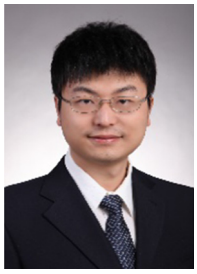

Bo Zeng (Member, IEEE) received a Ph.D. degree in electrical engineering from North China Electric Power University, Beijing, in 2014. He is working at NCEPU, Beijing. His research interests include integrated energy system optimization and power distribution system planning.

XinzhuXu received a B.S. degree in electrical engineering from North China Electric Power University, Beijing, China, in 2022. Her current research interests include energy system planning, emerging digital infrastructure planning, and electric vehicle integration.

FulinYang received a B.S. degree in electrical engineering from North China Electric Power University, Beijing, China, in 2021. His current research interest is integrated energy system optimization.